# Substrate Integrated Waveguide Couplers for Tapered Slot Antennas in Adaptive Receiver Applications

Lisa Locke[1,2], Zamzam Kordiboroujeni[1], Jens Bornemann[1], Stéphane Claude[2]
[1] Department of Electrical and Computer Engineering, University of Victoria, Victoria, BC, V8W 3P6, Canada
[2] Herzberg Institute for Astrophysics, Victoria, BC, V9E 2E7, Canada

***Abstract*—The design of substrate integrated waveguide couplers for adaptive receiver applications employing tapered slot antennas is presented. Two different 20 dB couplers are designed on low-permittivity substrate, and their performances are verified by commercially available field solvers. For an incident plane wave, the systems of antenna and couplers are demonstrated to provide the desired operation between 18 GHz and 28 GHz in terms of both received E-field levels and propagation through the components. Antenna radiation patterns are provided. Two different SIW coupler designs are compared with measurements and are found in good agreement, thus validating the design procedure.**

***Index Terms*— *substrate integrated waveguide; tapered slot antenna; directional coupler; adaptive receiver.***

## I. INTRODUCTION

In adaptive receiver systems, a part of the power captured by the antenna is coupled into limiter or gain control circuits that limit the power delivered to or drive the gain of the receiving amplifier. This principle is used in a variety of applications such as communication [1] and wireless systems [2], [3], RFID tags [4], distance sensors [5], and others. It is also used to limit the output power of transmitters [6].

Substrate integrated waveguide (SIW) technology is a promising trend in integrated receiver design [7]. Of the many planar antennas known, the antipodal tapered slot antenna (ATSA) is the obvious choice for connection with SIW circuitry, e.g. [8], [9].

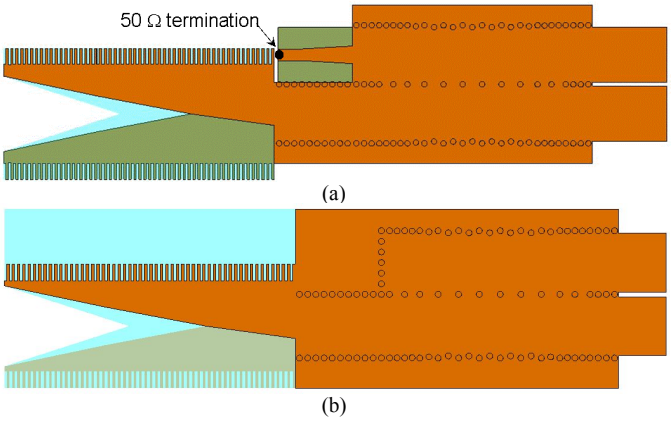


Figure 1. Antipodal linearly tapered slot antenna with substrate integrated waveguide coupler; isolated coupler port terminated (a) and shorted (b).

Therefore, this paper presents designs of two different SIW couplers to be used in adaptive ATSA-SIW receiver systems. The first approach is based on a four-port coupler whose performance depends largely on the requirement that all ports be matched. Therefore, in an actual design, the isolated port must be matched. As shown in Fig. 1a, this is commonly done by a SIW-to-microstrip transition terminated in a 50 Ω load which adds complexity to the fabrication process, especially in array applications.

The second approach uses a coupler that is used as an uneven power divider since its isolated port is shorted. The connection with the ATSA is shown in Fig. 1b. It is obvious that this circuit is readily mass-producible in standard printed-circuit technology. However, the disadvantage of this design, as discussed in the next section, is that the three divider ports cannot be simultaneously matched.

In the following Section II, we will first highlight the coupler designs and then verify the theoretical results with measurements for two previously published couplers. Section III presents the performance of the antenna, first in terms of radiation characteristics and then as a receiver system including the couplers.

## II. COUPLER DESIGN

The substrate selected for this application is RT/Duroid 6002 with $\varepsilon_r$=2.94, tanδ=0.0012, substrate thickness h=0.508mm, metallization thickness t=17.5µm, and conductivity $\sigma$=5.8x10$^7$S/m. For the design of the coupler and the SIW port of the antenna, the following parameters are used: via-hole diameters and center-to-center spacings are 642 µm and 866 µm, respectively. For a cutoff frequency of 14.05 GHz, the equivalent waveguide width is 6.22 mm and the SIW width 6.714 mm. The initial coupler design is accomplished in an all-dielectric waveguide environment by using well-known design procedures, e.g. [10]. In this step, certain dimensions pertaining to the SIW geometry are already fixed. They include parameters such as wall thickness, aperture width versus waveguide sections in the coupler, etc. This design is translated into an SIW coupler with square via holes which is analyzed and optimized by applying an efficient formulation of the mode-matching technique (MMT) [11] that uses square instead of circular via holes. After design specifications are met, the square vias are converted to circular ones [12] and designs verified by either CST Microwave Studio or HFSS.

This work is supported by the National Research Centre of Canada and the Natural Science and Engineering Research Council of Canada.

Fig. 2 shows the performance of a 20 dB SIW coupler with return loss and isolation better than 34 dB between 18 GHz and 27.3 GHz. Beyond this upper frequency, excitations of higher order modes in the coupler aperture sections limit the operation of the device. This behaviour is also known from H-plane waveguide couplers [10]. Narrowing the SIW guides would push the spikes beyond 28 GHz, but at the expense of increasing coupling values between 18 GHz and 21 GHz. The comparison between the results obtained with the MMT and CST are very good, with CST predicting about 0.35 dB more loss in the through port ($|S_{21}|$). If connected to the ATSA in Fig. 1a, such a system could be made adaptive for both RX and TX operations if the 50 Ω resistor would be replaced by a TX gain limiter.

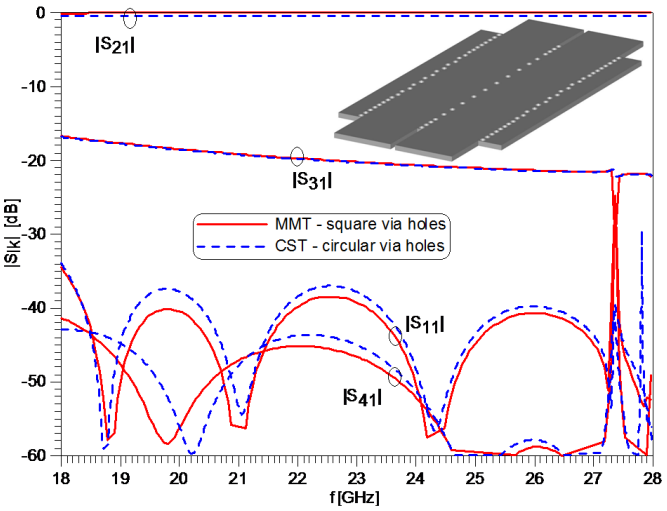


Figure 2. Performance of 20 dB SIW coupler and comparison between MMT (square via holes) and CST (circular via holes).

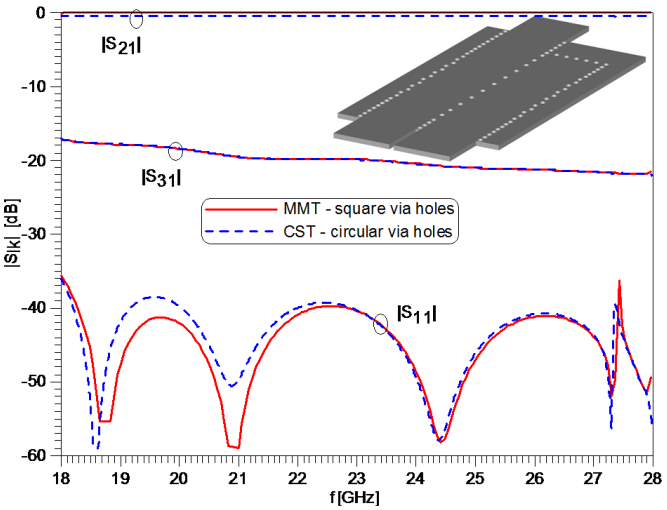


Figure 3. Performance of a 20 dB SIW coupler with a short on the isolated port and comparison between MMT (square via holes) and CST (circular via holes).

For an application in a receiver module, the isolated port of the coupler in Fig. 2 should ideally be matched. However, producing a match in SIW is not straightforward and would, as mentioned earlier, require fabrication steps in addition to the simple printed-circuit board process to fabricate the ATSA-coupler.

Therefore, it is more appropriate in SIW to short the isolated port. The performance of such a coupler is shown in Fig. 3. Very good agreement between the MMT and CST is observed, thus validating the design. In comparison with Fig. 2, it is obvious that the short reduces the level of spikes at around 27.3 GHz. However, it comes with the price of a poor match at the coupled port. This is of no concern as long as it can be accommodated by an Automatic Gain Control (AGC) circuit connected to that port. For comparison, the individual 3dB power dividers in SIW technology as used in, e.g., [9] have an output return loss in the order of 6 dB and operate well in a feed network for eight ATSAs.

In order to verify the coupler design procedure, results must be compared to measurements. Fig. 4 shows such a comparison for a 3 dB Ka-band SIW coupler. First of all, very good agreement between MMT (square vias) and CST (circular vias) is observed. The results are obtained using waveguide ports since experimental results reported in [13] are obtained by using calibration standards to reduce the influence of SIW-to-microstrip and microstrip-to-coaxial-end-launcher transitions. However, since only two of the four ports are deembedded simultaneously, the coaxial loads on the other two ports influence the measurement. This explains the differences in $|S_{11}|$ and $|S_{41}|$ between simulations and measurements. Within the operating frequency band, the overall agreement is good, and the measured return loss is better than 20 dB over most of the 26 – 34 GHz range.

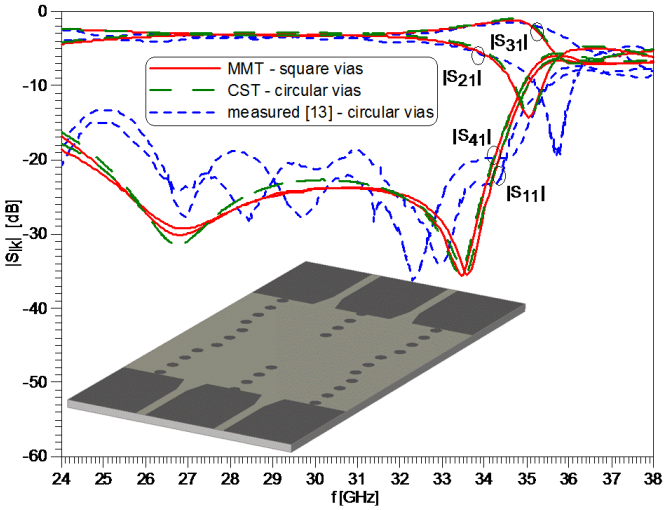


Figure 4. Performance comparison between results obtained with MMT (square via holes – solid lines), CST (circular via holes – dashed lines) and measurements (circular via holes – dotted lines) for a 3dB Ka-band SIW coupler according to [13].

A comparison for a 3 dB coupler with microstrip ports is presented in Fig. 5. The measured data in [14] is obtained with microstrip-to-coaxial end launchers which are not included in the simulations. Nevertheless, the agreement between experimental and simulated results is quite good with simulations and measurements showing input return loss and isolation values better than 10 dB between 8 GHz and 12.5 GHz. The differences between MMT (square vias) and CST

(circular vias) results are attributed to the modelling of the SIW-to-microstrip transitions. While CST models the microstrip taper as seen in the inset of Fig. 5, the MMT code uses a staircase approximation [11, 12] of ten steps in this case.

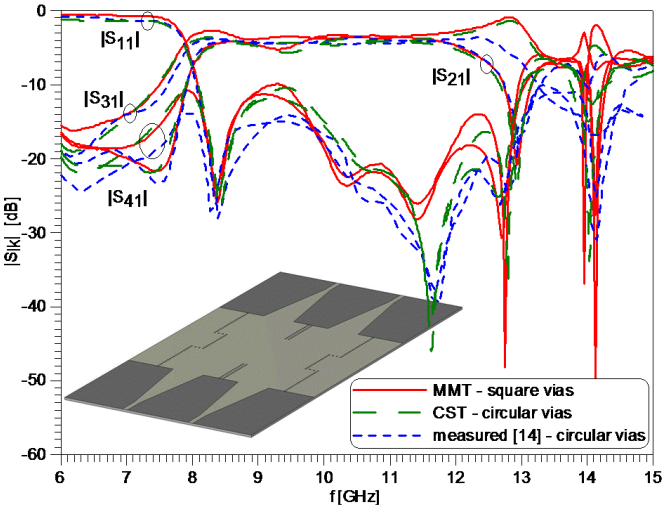


Figure 5. Performance comparison between results obtained with MMT (square via holes – solid lines), CST (circular via holes – dashed lines) and measurements (circular via holes – dotted lines) for a 3dB Ka-band SIW coupler according to [14].

This completes the coupler design and validation section. We now proceed with the antenna system of ATSA and SIW couplers.

## III. Antenna System

The ATSA is designed following basic guidelines presented in [16] with the substrate cut out close to the aperture to satisfy the effective thickness requirement [16]. Corrugations are added to limit the overall height of the antenna and to improve cross polarization [17]. The radiation pattern of the antenna system is presented in Fig. 6 for three different frequencies – 20 GHz (Fig. 6a), 23 GHz (Fig. 6b), and 26 GHz (Fig. 6c). This ATSA features a pattern that is narrower in the E-plane than in the H-plane. Other combinations depending on antenna length, taper function, etc, are possible [18]. Fig. 6 demonstrates the wide band characteristic of the antenna. Between 20 GHz (Fig. 6a) and 26 GHz (Fig. 6c), the E-plane half-power beam width varies between 42 and 39.5 degrees, the H-plane half-power beam width between 66 and 59 degrees, and the maximum observed cross-polarization level at 45 degree (within the 3 dB E-plane beam width) increases from 25 dB at 20 GHz to 18 dB at 26 GHz.

In order to demonstrate the capabilities of the combined ATSA coupler system in a receiver scenario, Fig. 7a shows the performance of the system in Fig. 1a when a plane wave with amplitude of 1V/m is excited in the far field of the antenna. Due to its small size, the antenna captures only a small part of the plane wave (around -60 dB) and provides signals at output port 1 (through) and port 2 (coupled). Fig. 7a shows their individual levels versus frequency and the ratio of the output signals. It is observed that both the coupled and through ports experience some fluctuation of levels. This is attributed to two

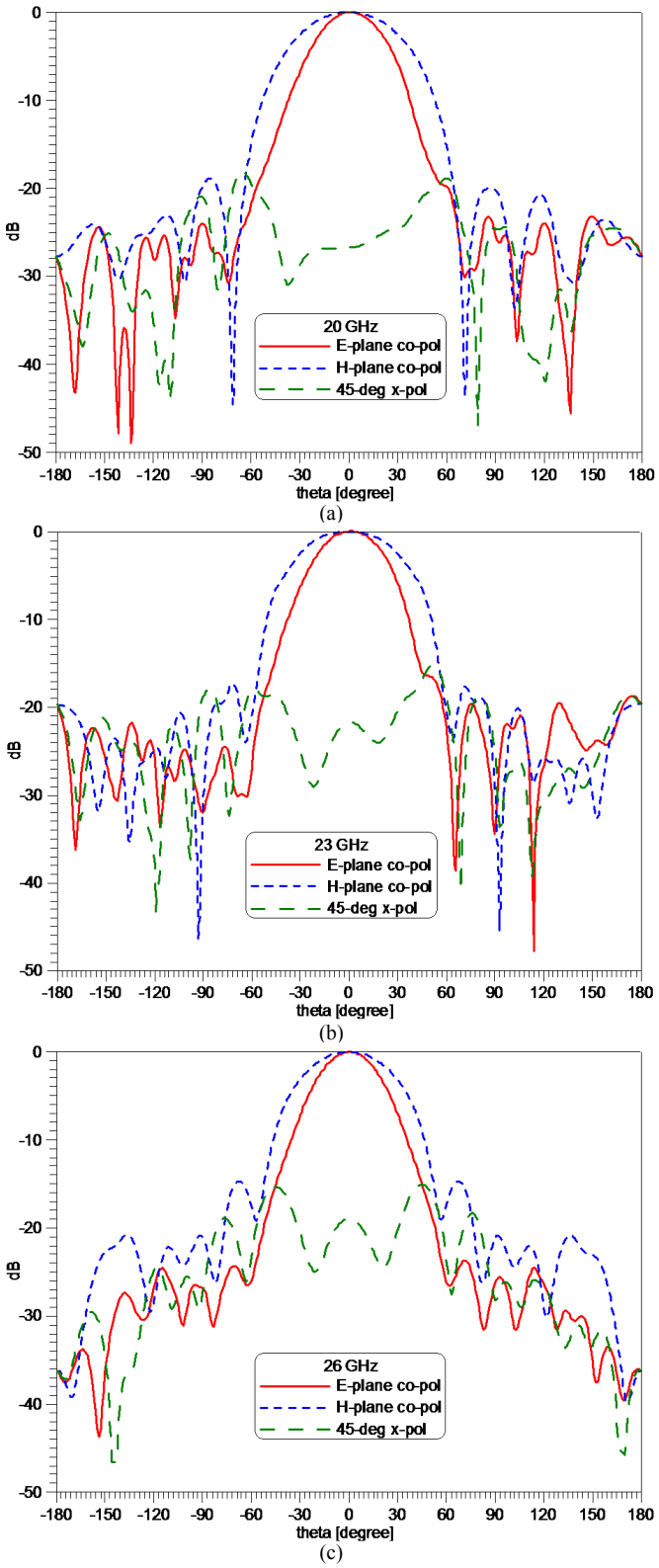


Figure 6. Principle-plane co-polarized and 45-degree cross-polarized radiation pattern of the ATSA at selected frequencies; (a) 20 GHz, (b) 23 GHz, (c) 26 GHz.

factors: first, the SIW-to-microstrip transition and its 50 Ω termination cause some reflection that propagates through the

system and impacts the system performance mostly at the level of lowest signal (port 2); secondly, as the plane wave excites the ATSA and propagates through the system in Fig. 7b, a small amount of electric field is observed at the location of the 50 Ω termination (c.f. inset of Fig. 7a). This field adds another, unwanted input to the coupler which deteriorates its performance. Note that the magnitude of the total field at port 3 ($E_3$ in Fig. 7a) can even be higher than the one at the coupled port (e.g. at 22.5 GHz).

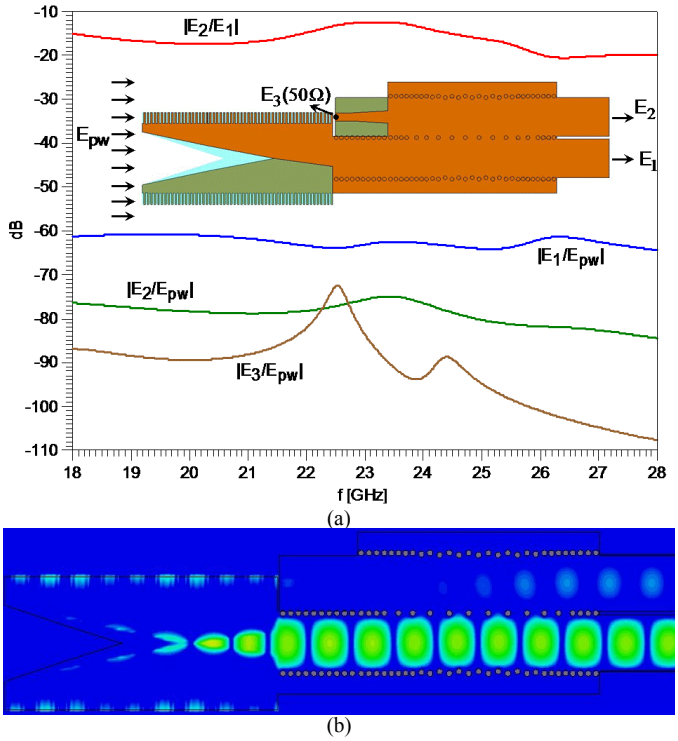


Figure 7. Performance of the system of Fig. 1a when excited in the far field by a plane wave (pw) of 1V/m magnitude; (a) E-field amplitudes in dB, (b) propagation through the system at 23 GHz.

For comparison, Fig. 8a shows the same analysis for the system in Fig. 1b using the shorted coupler as unequal power divider. Note that the fluctuations at the coupled port are drastically reduced and that the ratio between the two output ports 1 and 2 is almost identical to that of the coupled port ($|S_{31}|$) in Fig. 3, thus validating the design of the coupler. Fig. 8b depicts a snapshot of E-field propagation through the antenna system when a plane wave is incident at the antenna port. Together with Fig. 8a, it demonstrates that the system operates according to specifications and that it can be used in adaptive receiver applications. Of course, SIW couplers with other coupling factors can be designed according to [12] if required.

## IV. CONCLUSIONS

Substrate integrated waveguide couplers present a viable option for adaptive receivers using antipodal tapered slot antennas. Two examples of 20 dB couplers are presented: one four port coupler for adaptive transmit and receive operations and a three port coupler for receive operation only. In a receiver application connecting the ATSA to the coupler, the four port coupler fails to receive a flat frequency response due to the fact that first, the isolated port has to be terminated and secondly, that an incoming plane wave will excite a small signal at the terminated port. In comparison, the coupler operating as an unequal power divider achieves an excellent response over the entire 18 GHz to 28 GHz bandwidth but suffers from a limited match at the coupled port. If such a change in impedance level can be accommodated in an automatic gain control circuit within a receiver, then the antenna system using the coupler as an unequal power divider (Fig. 1b) is the preferred system due to its flatter performance over a wide frequency band.

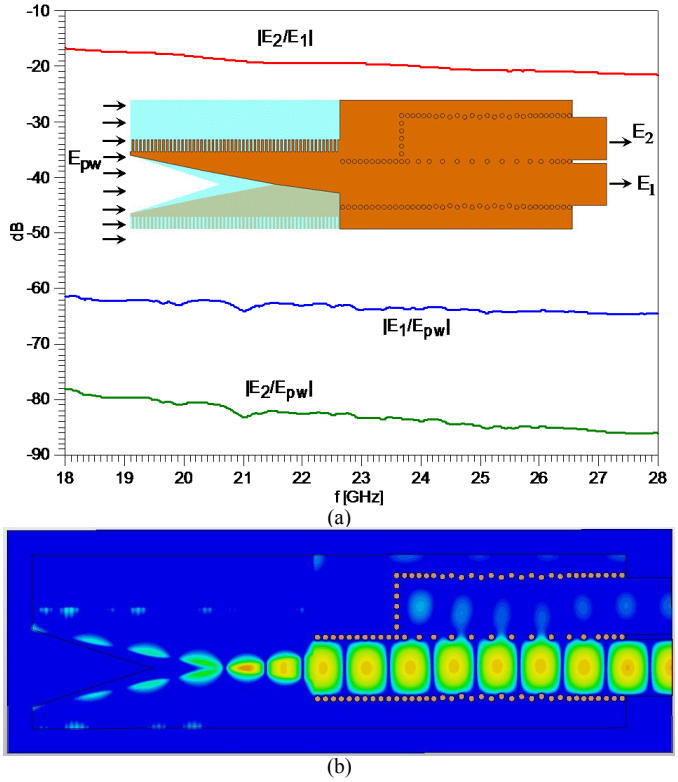


Figure 8. Performance of the system of Fig. 1 when excited in the far field by a plane wave (pw) of 1V/m magnitude; (a) E-field amplitudes in dB, (b) propagation through the system at 23 GHz..

## REFERENCES

[1] R. Popovich, "Receiver protection considerations for T/R modules employed in AESA systems," Proc. IEEE Int. Conf. Microwaves, Communications, Antennas and Electronic Systems (COMCAS), pp. 1-4, Tel-Aviv, Israel, May 2008.

[2] U. Alvarado, N. Rodriguez, J. Mendizabal, R. Berenguer, and G. Bistue, "A dual-gain ESD-protected LNA with integrated antenna sensor for a combined GALILEO and GPS front-end," Proc. Topical Meeting Silicon Monolithic Integrated Circuits in RF Systems, pp. 99-102, Long Beach, USA, Jan. 2007.

[3] S. Lim, K.M.K.H. Leong, and T. Itoh, "Adaptive power controllable retrodirective array system for wireless sensor server applications," IEEE Trans. Microwave Theory Tech., vol. 53, pp. 3735-3743, Dec. 2005.

[4] G.K. Balachandran and R.E. Barnett, "A passive UHF RFID demodulator with RF overvoltage protection and automatic weighted threshold adjustment," IEEE Trans. Circuits Systems, Pt. I, vol. 57, pp. 2291-2300, Sep. 2010.

[5] I. Sarkas, J. Hasch, A. Balteanu, and S.P. Voinigescu, "A fundamental frequency 120-GHz SiGe BiCMOS distance sensor with integrated antenna," IEEE Trans. Microwave Theory Tech., vol. 60, pp. 795-812, Mar. 2012.

[6] J.I. Garatel, J.J. Zamora, J. M. de Diego, and L. Gonzalez, "RF output power sensing for low power transmitters in mobile base stations based on antenna switch isolation losses," Proc. IEEE Int. Symp. Industrial Electronics, vol. 2, pp. 1053-1056, Ajaccio, France, May 2004.

[7] K. Wu, "State-of-the-art and future perspective of substrate integrated circuits (SICs)," in Workshop Notes: Substrate Integrated Circuits, IEEE MTT-S Int. Microwave Symp., Anaheim, USA, May 2010.

[8] Z.C. Hao, W. Hong, J.X. Chen, X.P. Chen, and K. Wu, "A novel feeding technique for antipodal linearly tapered slot antenna array," IEEE MTT-S Int. Microwave Symp. Dig., pp. 1641-1643, Long Beach, CA, June 2005.

[9] S. Lin, S. Yang, A.E. Fathy, and A. Elsherbini, "Development of a novel UWB Vivaldi antenna array using SIW technology," Progress In Electromagnetics Research, PIER 90, pp. 369–384, 2009.

[10] J. Uher, J. Bornemann, and U. Rosenberg, Waveguide Components for Antenna Feed Systems. Theory and CAD. Artech House Inc., Norwood 1993.

[11] J. Bornemann, F. Taringou, and Z. Kordiboroujeni, "A mode-matching approach for the analysis and design of substrate-integrated waveguide components," Frequenz J. RF/Microwave Engr. Photonics, Communications, vol. 65, pp. 287–292, Sep. 2011.

[12] Z. Kordiboroujeni, J. Bornemann, and T. Sieverding, "Mode-matching design of substrate-integrated waveguide couplers," Proc. Asia-Pacific Int. Symp. Electromagnetic Compatibility, pp. 701-704, Singapore, May 2012.

[13] Y. Cassivi, D. Deslandes, and K. Wu, "Substrate integrated waveguide directional couplers," Proc. Asia-Pacific Microwave Conf., pp. 1409-1412, Kyoto, Japan, Nov. 2002

[14] J.-X. Chen, W. Hong, Z.-C. Hao, H. Li, and K. Wu, "Development of a low cost microwave mixer using a broad-band substrate integrated waveguide (SIW) coupler," IEEE Microwave Wireless Comp. Lett., vol. 16, pp. 84–86, Feb. 2006.

[15] J.-X. Chen, W. Hong, Z.-C. Hao, H. Li, and K. Wu, "Development of a low cost microwave mixer using a broad-band substrate integrated waveguide (SIW) coupler," IEEE Microwave Wireless Comp. Lett., vol. 16, pp. 84–86, Feb. 2006.

[16] K.S Yngvesson, D.H. Schaubert, T.L. Korzeniowski, E.L. Kollberg, T. Thungren, and J. F. Johansson, "Endfire tapered slot antennas on dielectric substrates," *IEEE Trans. Antennas Propagat.*, vol. 33, pp. 1392-1400, Dec. 1985.

[17] H. Sato, Y. Takagi, and K. Sawaya, "High gain antipodal Fermi antenna with low cross polarization," IEICE Trans. Commun., vol. E94-B, pp. 2292-2297, Aug. 2011.

[18] K.S. Yngvesson, T.L. Korzeniowski, Y.-S. Kim, E. Kollberg, and J.F. Johansson, "The tapered slot antenna - A new integrated element for millimeter wave applications," IEEE Trans. Microwave Theory Tech., vol. 37, pp. 365-374, Feb. 1989.